Application of Digital Design Technology in the Design of Intelligent Mechanical Equipment

Qiujing Meng[1]

[1] Sino-German Institute of Engineering, Shanghai Technical Institute of Electronics & Information, Shanghai, 201411, China, mengqiujing8@126.com

Corresponding author: Qiujing Meng, mengqiujing8@126.com

Abstract: The design capability of intelligent mechanical equipment is an important driving force for the high-quality development of the manufacturing industry. Against the backdrop of the rapid development of digital technology and computer networks, modern digital design technology has become the direction of intelligent mechanical equipment design. However, currently, a large number of manufacturing industries in China are still dominated by traditional manufacturing models, and digital design is rarely applied due to its complex technology and high initial costs. To promote the high-quality development of the manufacturing industry and optimize digital design technology, this study adopts an optimization algorithm based on object detection and 3D information measurement to construct an operating system for digital technology design in intelligent mechanical equipment design. The results show that compared with the algorithms proposed by YOLO, YOLO-2, and YOLO-3, this algorithm has better stability and speed in iteration, and the 3D recognition error is controlled within 4%. This study innovatively applies digital design technology to the design of intelligent mechanical equipment, not only providing reference and data support for the improvement direction of digital design technology, but also providing new path choices for the design of intelligent mechanical equipment.

Keywords: Intelligent mechanical equipment design; Digital design; Object detection; 3D information measurement.
DOI: https://doi.org/10.14733/cadaps.2024.199-214

1   INTRODUCTION

In the modern society of information technology, with the continuous growth of manufacturing, the traditional mechanical equipment design (MED) technology has been difficult to meet the current large demand for mechanical equipment in the manufacturing industry [1]. After continuous reform and innovation, intelligence and diversification have become one of the most important directions in the manufacturing industry at present. China's manufacturing industry is currently promoting industrial technology change, with the aim of integrating digital design technology into

the field of intelligent MED, to promote the high-quality development of manufacturing and people's living standards [2]. Digital design technology mainly integrates technologies such as the Internet, computer networks, and robotics to simulate and model mechanical products according to the needs of users to produce the required mechanical products [3]. Traditional MED technology, due to the limitations of technology, tools, and thinking, makes the design inadequate and unspecific, resulting in many mistakes. Compared with traditional MED, modern digital technology has the advantages of a short design cycle, more flexible design, and integration [4]. In this context, the main objective of this study is to optimize and innovate digital design techniques and to explore their application in intelligent MED. The study aims to optimize digital technologies through object detection (OD) and 3D information measurement techniques for more efficient and accurate intelligent MED. This move is not only expected to enhance the capability of digital design techniques, but also to provide more innovative and efficient smart machinery solutions for the manufacturing industry. By analyzing and validating the performance of optimization algorithms based on OD and 3D information measurement for intelligent MED, this study aims to contribute to the knowledge base in intelligent manufacturing and provide a basis for further research and applications in related fields.

2   RELATED WORKS

With the spread of digital technology and computer networks, there has been a strong impact on the manufacturing industry. Within the manufacturing industry, the increasing demand for efficiency in production processes and product quality has necessitated the need for constant updating and upgrading of technical equipment. To achieve the intelligence of machinery and equipment, there is a need to integrate various digital design techniques. Therefore, a large number of scholars at home and abroad have conducted a lot of research on digital technology and intelligent MED. Ae A et al. studied the crystallization of commercially active pharmaceutical ingredients and optimized the algorithms for kinetic related parameters based on digital design. The concentration, particle size and other traits of the chemically synthesized products were fitted. The experimental findings denoted that the model developed in the study was able to predict various traits of the products with high accuracy. Finally, the model was used in a dynamic optimization framework for digital design, which contributed greatly to the quality of the product data [6]. Cheung K L et al. applied digital design to people's mental health interventions by first selecting a theoretical model and then developing intervention goals for digital design. Through qualitative and quantitative analysis, salient features were identified, and finally, intelligent algorithms and intervention programs were designed. The research outcomes indicated that the digital design model proposed in the study was able to provide an accurate intervention plan with good application value [7]. Zhou J et al. used the roots of plants as bio-design materials for making self-supporting 3D structures. Biomaterials and digitally designed materials provide stability to each other. The digital design technique enabled a better understanding and prediction of the repair activity of plant roots. It was a great contribution to the setting of key parameters for experiments and to the development of the structural potential of plant roots [8]. Makaremi M et al. applied digital design to the design of 21st century cosmetic dentistry and prosthetic rehabilitation with the aim of linking the initial situation of the patient to the final outcome for treatment project for better planning. The findings of the study expressed that in practical application, the research design approach was good and relevant in helping the patients to treat well [9].

As the advancement of science and technology, the YOLO algorithm has received many improvements and applications in OD. Choudhary M et al. introduced a new framework model that utilized the YOLO algorithm to locate regions and used it for image selection and core texture detail processing. The research outcomes indicated that the YOLO method could accurately limit the iris region without loss and effectively reduce the error of existing technologies, to some extent, relieving the threat of forged iris confusion recognition systems [10]. Shen H et al. proposed a method for extracting building roofs from echo images to improve the speed of

geographic information extraction and data collection. The research adopted and aggregated modules to improve the YOLOv5 algorithm. The experimental findings denoted that the improved YOLOv5s algorithm could achieve an average accuracy value of 95.3%, and the CPU used could reach 11.75 frames per second, making it more efficient to obtain building roofs from images [11]. Especially in the research of robotic arms, YOLO algorithm has achieved many results. The Dashygenis M was based on the Niryo One robotic arm and was equipped with a universal serial bus and high-definition camera in the end effector, thereby improving the accuracy of operation. In algorithm optimization, this study was based on the YOLO algorithm and added new feature calculation steps for the construction of motion models. In the laboratory, research has proven the effectiveness of this method, and the accuracy of the robotic arm in detecting and transmitting objects has reached 96.66% [12]. Li D et al. proposed a YOLOv3 based OD control method for grasping problems with complex geometric features and chaotic backgrounds, and applied it to the spring robot grasping system. The YOLOv3 OD model was used to detect and locate objects, and then based on corner features, a robot attitude controller was designed. This method adopted a convergence alignment grabbing control strategy to achieve grabbing and has strong robustness. The research findings of localization and grabbing show that this method could achieve automatic localization and grabbing in complex geometric features and cluttered backgrounds, and had strong robustness to changes in lighting [13].

In summary, due to the unique advantages of digital technology, it has been widely used and developed in various disciplines [14]. However, the application of digital technology in the field of intelligent MED is still small. If the digital technology and intelligent MED can be well combined, the manufacturing efficiency and quality will be better improved. Therefore, this study proposed digital technology based on OD and 3D information measurement for the motion planning of robotic arms in intelligent MED. It aims to increase the efficiency of design and manufacturing and create conditions to promote the economic development of China. However, through the review of existing literature, several gaps can be identified. First, there is limited research on the integration of digital design technology with intelligent MED, as most of the studies focus on specific areas such as pharmaceuticals, mental health interventions, and packaging. Second, while there has been some focus on the application of algorithms like YOLO for OD, the emphasis on how digital design technologies can specifically enhance manufacturing efficiency in intelligent mechanical systems is not substantial. Third, there is an absence of holistic approaches in the literature that combine different digital design technologies for the intelligent MED. Lastly, although research on OD and manipulation through robotic arms is available, the incorporation of digital design to tackle complex geometric features and environmental constraints in intelligent MED is underrepresented. These gaps in the literature highlight the need for more comprehensive research on the application of digital design technology in intelligent MED. There is a significant potential in integrating various technologies to address specific challenges in manufacturing efficiency and environmental constraints. This study aims to address these gaps by proposing a novel approach that combines digital technology with intelligent MED.

3 OPTIMIZATION OF DIGITAL TECHNOLOGY AND INTELLIGENT MECHANICAL DESIGN MODELING

3.1 Digital Design Techniques based on Deep Learning Improvements

Digital design is the combination of digital technology and design, which shows human's various ideas and plans through the way of computer technology. With the rapid development of computer technology, more algorithm tools are used in design. This study combines OD algorithms and 3D information measurement techniques in deep learning to improve digital design. Digital design technology in intelligent MED, research on object recognition and classification is developing rapidly. The OD algorithm has become the mainstream method of recognition and classification, among which the You Only Look Once (YOLO) algorithm model as the most representative single-stage OD algorithm has good detection accuracy and excellent detection rate [15]. Therefore, this

study uses the YOLO algorithm model as a network model for OD and classification to enable intelligent design of mechanical equipment to be identified autonomously, and to perform 3D calculations and determine the coordinates of object centroids based on the OD region of the model combined with the distance information collected by the depth camera [16]. YOLO is an algorithm model for end-to-end OD based on the CNN model. The YOLO model treats the OD problem as a regression problem, and the solution process divides the input image information into cells of the same size, and each cell is detected independently, thus completing the calculation of the location and type of the object in the image from the input unprocessed image to the output object [17]. In the network design, the YOLO algorithm model has a total of 24 convolutional layers and 2 fully connected layers, and the specific structure is shown in Figure 1.
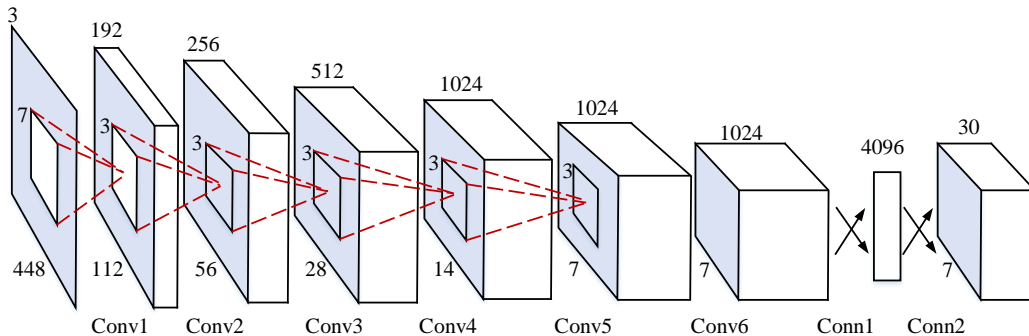
Figure 1: Structure diagram of YOLO algorithm model.

The first 20 convolutional layers in the network, plus an average pooling layer and a fully connected layer, are used in the training of the YOLO algorithm model as the training network. Then, those 4 convolutional layers and 2 fully connected layers are used to output the OD region coordinates along with the output concept. Relative to the initial YOLO algorithm, second generation YOLO algorithm (YOLO-2) uses a new base network model, Darknet-19 (D19), consisting of 19 convolutional layers and 5 maximum pooling layers. D19 uses 3 × 3 convolution and 2 × 2 maximum pooling to halve the dimensionality of the feature image and double the number of channels of the feature map. D19 finally uses global average pooling to predict, while YOLO-2 adds a normalization layer after the convolution layer to speed up convergence and prevent overfitting in this way. The training of YOLO-2 consists of three stages. The first stage is the pre-training of the model, at which point the model input is 224 × 224 and the samples are trained 160 times. The second stage adjusts the network input, at which point the model input is 448 × 448 and the samples are trained 10 times. The third stage uses the classification model as a detection model, and is continuously tuned on the dataset to obtain the optimal detection model. The main advantage of YOLO-2 is the inclusion of a batch normalization (BN) layer in the network structure. The original features of the data are preserved while simplifying the data distribution of the neural network. The output data in the BN algorithm is calculated as shown in equation 3.1.

$$Z_N = W_N * A_{N-1} + b_N \tag{3.1}$$

In equation (1), Z_N denotes the output data of the N layer; W means the output weights; A_{N-1} refers to the activation result of the $N-1$ layer1; b expresses the distribution bias of the data. Assuming that the output of the n th neural node of the current layer is Z_n, and the batch size of the training sample of the N th layer is m, the mean and variance of Z_n can be obtained as shown in equation 3.2.

$$\begin{cases} \mu = \dfrac{1}{m} \sum_{N=1}^{m} Z_n^N \\[2mm] \sigma^2 = \dfrac{1}{m} \sum_{N=1}^{m} (Z_n^N - \mu)^2 \end{cases} \tag{3.2}$$

Using the mean and variance found in equation 3.2, the new output $\hat{Z}_n$ can be calculated as shown in equation 3.3.

$$\hat{Z}_n = \frac{Z_n - \mu_n}{\sqrt{\sigma_n^2 + \varepsilon}} \tag{3.3}$$

In equation (3.3), ε refers to the fixed-value parameter to prevent the generation of invalid variance, and $\hat{Z}_n$ means the new output result obtained, by which the normalization of the data is completed. Therefore, each feature distribution of the input has a mean of 0 and a variance of 1. At this point, to prevent the loss of learning parameters of the underlying network from occurring by changing the information representation of the original data through the transformation operation, the study introduces the learnable parameters α and β. The linear transformation is performed on the normalized data as shown in equation (3.4).

$$\hat{Z}_n = \alpha_n * \hat{Z}_n + \beta_n \tag{3.4}$$

When equation 4 is satisfied by both $\alpha^2 = \sigma^2$ and $\beta = \mu$, the BN algorithm can retain the distribution information of the original input features and achieve the equivalent transformation. The advantages of the BN algorithm are that it can make the distribution of the input data in each layer of the network relatively stable, which can effectively increase the training speed of the algorithm model, reduce the negative impact of the parameters on the algorithm model, making the training process more stable. Besides, it is compatible with saturation activation function, and can reduce the gradient disappearance and prevent the training process over-fitting. This study uses an improved algorithm based on YOLO and YOLO-2, called the YOLO-3 algorithm. The structure of the YOLO-3 network is shown in Figure 2.
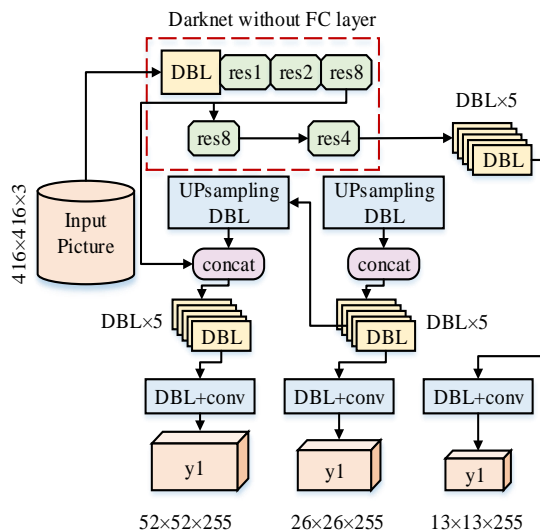
Figure 2: Network structure of YOLO-3.

In Figure 2, "DBL" is the basic component of YOLO-3, including convolution, BN algorithm and Leaky Relu function, and the number of BN and Leaky Relu layers is the same in the network structure of YOLO-3. The main improvements are that the backbone network is modified to Darknet-53 and a new residual network structure is added. The residual network structure improves the correctness of the model by increasing the depth and alleviates the gradient disappearance problem in the original model as the amount of network layers increases. The residual network structure is shown in Figure 3.
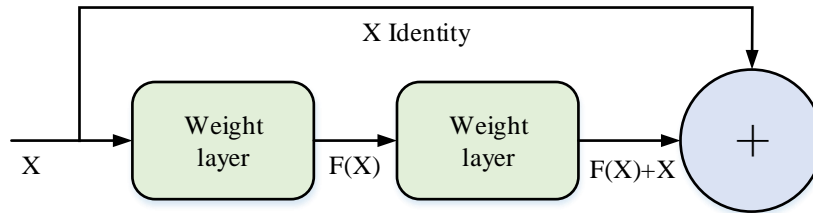
Figure 3: Residual network structure diagram.

In the improved YOLO-3 algorithm model, the calculation of the loss function can be divided into coordinate loss, confidence loss, and classification loss. The equation for their calculation is shown in equation (3.5).

$$Loss = 0.5 \times \sum_{i=1}^{K} \lambda_{obj} \left\{ (2-t_h)^2 \times \sum_{r \in (x,y,w,h)} (t_r - p_r)^2 \right\} + (t_{conf} - p_{conf})^2 + $$

$$0.5 \times \sum_{i=1}^{K} \lambda_{obj} \left\{ \sum_{r=0}^{N-1} \left[(r = t_{class})?1:0 - p_{classr} \right]^2 \right\} \tag{3.5}$$

In equation (5), $Loss$ denotes the coordinate loss, the error between the predicted bounding box and the real bounding box; p_h and p_w express the height and width of the predicted bounding box; t_h and t_w indicate the size of the actual bounding box where the object is located; (x, y) refers to the coordinate point of the center of the box, so it is known that the center point coordinates of the object's real location box are (t_x, t_y) and the center coordinates of the predicted bounding box are (p_x, p_y). K expresses the output quantity under different image sizes; λ_{obj} means the object coefficient. The specific calculation is shown in equation (3.6).

$$\begin{cases} \lambda_{obj} = 1, \text{ if object exists} \\ \lambda_{obj} = 0, \text{ otherwise} \end{cases} \tag{3.6}$$

To enhance the accuracy of the prediction bounding box generation, the study incorporates $2 - t_w \times t_h$ as a penalty factor for large bounding box errors in YOLO-3. The activation function uses the Sigmoid function to keep the network predictions in the interval of 0 to 1. The Sigmoid function expression is shown in equation (3.7).

$$S(t) = \frac{1}{1+e^{-1}} \tag{3.7}$$

The activation function processing enables to reduce the deviation between the predicted bounding box and the actual bounding box. The mean square error between the bounding boxes is then used to calculate the coordinate loss, and the expression is shown in equation (3.8).

$$L_1 = 0.5 \times \sum_{i=1}^{K} \lambda_{obj} \times \left[(2 - t_w \times t_h)^2 \times \sum_{r \in (x,y,w,h)} (t_r - p_r)^2 \right] \tag{3.8}$$

In the calculation of classification loss, the traditional Softmax algorithm is changed to a logic classifier to accomplish multi-objective classification. The classification function is calculated using a dichotomous cross-entropy function, whose expression is shown in equation (3.9).

$$L_2 = 0.5 \times \sum_{i=1}^{K} \lambda_{obj} \times \left[\sum_{r=0}^{N-1} \left[(r = t_{class})?1:0 - p_{classr} \right]^2 \right] \tag{3.9}$$

The loss of confidence is calculated as shown in equation (3.10).

$$L_3 = (t_{conf} - p_{conf})^2 \tag{3.10}$$

In equation (3.10), t_{conf} denotes the object true border confidence and p_{conf} means the object predicted border confidence.

3.2 Robotic Arm Calibration and Motion Planning in Intelligent MED

In the design of intelligent mechanical equipment, the calibration and motion planning of the robotic arm is crucial. By using digital design techniques such as high precision sensor data processing and complex algorithms, it is able to calibrate the position of the robotic arm more accurately. At the same time, digital tools allow us to create more complex and flexible motion planning to adapt to changing work environments and task requirements. These digital technologies provide powerful support for optimizing the performance of robotic arms and are a key component of intelligent MED. This research applies MoveIt motion planning software to build a three-dimensional model of the robot arm, which not only enables control of the robot arm, but also obstacle avoidance and motion planning. The overall structure of MoveIt is shown in Figure 4.
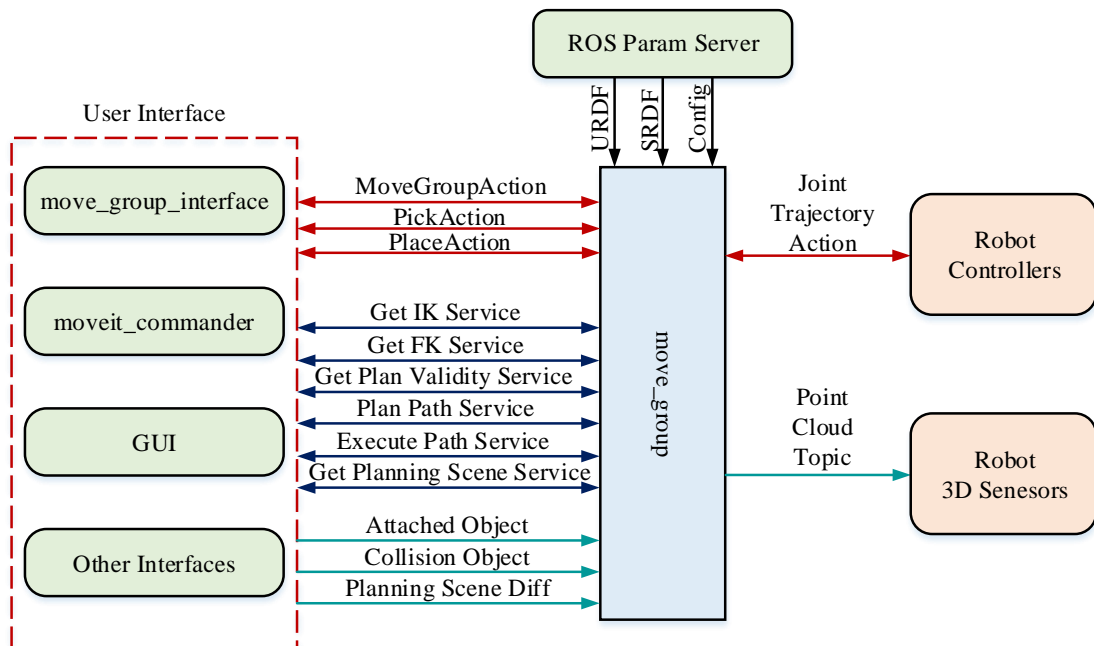

Figure 4: MoveIt general structure diagram.

In the process of equipment design and manufacturing of robotic arm, first of all, hand-eye calibration is required to accurately grasp the object and realize the transformation of camera coordinate system to robotic arm coordinate system. Hand-eye calibration is divided into two forms, depending on where the camera is fixed, if the camera and the end of the robot are fixed together, it is called eye in hand, and if the camera is fixed on the base outside the robot, it is called eye to hand [18]. At this stage, in the intelligent mechanical operating system, the more applied depth camera technology is the binocular stereo depth vision camera [19]. The basic principle is that by two same-plane cameras, the same object is photographed, and then the image is calibrated and matched by the parameters inside and outside the camera, and the depth information is obtained according to the matching result. The expression of the calculation is shown in equation (3.11).

$$z = \frac{f \times b}{X_l - X_r} \qquad (3.11)$$

In equation (3.11), z denotes the length of the object on the vertical axis from the horizontal line of the camera focal length; x refers to the distance of the object on the horizontal axis from the left camera; f expresses the camera focal length; b means the baseline length; X_l denotes the horizontal offset of the left camera; X_r indicates the horizontal offset of the right camera. The ideal model is shown in Figure 5.
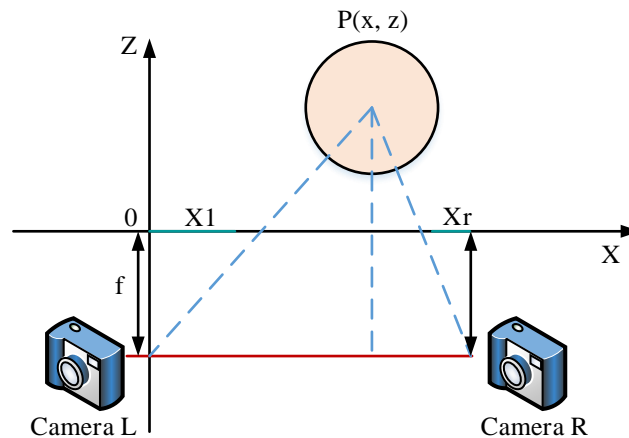
Figure 5: Calculation diagram of binocular stereo depth camera.

From equation (11) and Figure 5, the dual camera can obtain the depth information by calculating the parallax magnitude z, which is computationally inexpensive and widely used in the practical application. However, in practical situations, the large variation of natural light may lead to large differences between the images captured by the left and right cameras, and the requirements of the image feature matching algorithm increase subsequently, resulting in a single operating environment, which may lead to large errors. In the hand-eye calibration, the main position relationships considered, including the robot arm base, camera position, actuator position and calibration plate, are the conversion relationships between the coordinate systems in the case of the origin, respectively. The expression for defining the position of the calibrator in the coordinate system of the robot arm base is D, as shown in equation (3.12).

$$D = L \times M \times N \qquad (3.12)$$

In the coordinate system of the robot arm base, the robot arm base and the calibrator are fixed positions, so the D value is constant. And in the motion of the robot arm, the end position of the

robot arm is relatively constant with the camera position, so only the robot arm position needs to be changed to ensure that the object can be seen by the camera at both positions. The expression of the relationship between the two sets of positions is obtained, as shown in equation (3.13).

$$\begin{cases} D = L_1 \times M \times N_1 \\ D = L_2 \times M \times N_2 \end{cases} \qquad (3.13)$$

This study uses Time of Flight (TOF) technology to improve the traditional depth camera. The most important feature of TOF technology is the active detection method, which calculates the depth by comparing the change of the emitted light with the received light. The TOF camera selects the received light with the same wavelength of the emitted light by filtering device, and multiple shutters are applied to ensure the complete acquisition of the beam. Finally, the collected data is calculated by the computing system to get the distance information. The distance is calculated as shown in equation (3.14).

$$d = c \times t_d \times 0.5 \qquad (3.14)$$

In equation (3.14), the time from the emitted beam to the received beam is t_d, and c is the speed of light. Since t_d cannot be calculated directly, the study calculates the distance information by collecting the charge percentage, and the expression is shown in equation (3.15).

$$d = \frac{c}{2} \times \frac{S_1}{S_0 + S_1} \times t_p \qquad (3.15)$$

In equation (3.15), c represents the beam; t_p expresses the duration of the beam pulse; S_0 refers to the amount of charge collected earlier; S_1 means the amount of charge collected delayed. When the full charge is collected during the previous shutter and not during the next, $S_1 = 0$, the measured distance d = 0. When the full charge is not collected during the previous shutter and not during the next, $\frac{S_1}{S_1 + S_0} = 1$, and the equation (15) becomes $d = c \times t_p \times 0.5$. It is known that the maximum value of the measured distance in TOF technique is determined by the size of the t_p value, the longer the duration of the beam pulse, the larger the camera measurement range. Therefore, this study first establishes a 3D coordinate system with the robot arm base as the origin, and enters the environmental information into the coordinate system. Images and colors are captured by a depth camera modified by TOF technology. The information of the captured data is identified and classified at the control center. If the acquisition result is not the grasping object, the robotic arm is not operated. if the acquisition result is consistent with the grasping object, the control center gets the 3D information of the object by the algorithm proposed in this study. Through the obtained three-dimensional information and the coordinates of the object center point, the control center gives the grasping command to the robotic arm to realize the grasping operation of the object. The fast-extended random tree algorithm is also added in this study. In this method, the starting point is set as the origin, the random probability and fixed step size are used for rapid expansion, and the path and obstacle detection are carried out synchronously, and the final motion planning is obtained through iteration. The operation flow of the system designed in this study is shown in Figure 6.

4   EXPERIMENTAL ANALYSIS OF OPTIMIZED DIGITAL ALGORITHMS AND INTELLIGENT MECHANICAL DESIGN MODELS

In this study, five objects of different three-dimensional sizes were selected and sample pictures were collected by RGB three-color cameras. A total of 1000 sample pictures were obtained as the

training data set of the algorithm model. The change curves of the training loss values for YOLO-2 and YOLO-3 algorithms, which is improved in this study, for model training, using the same data set and under the same experimental conditions, are shown in Figure 7.
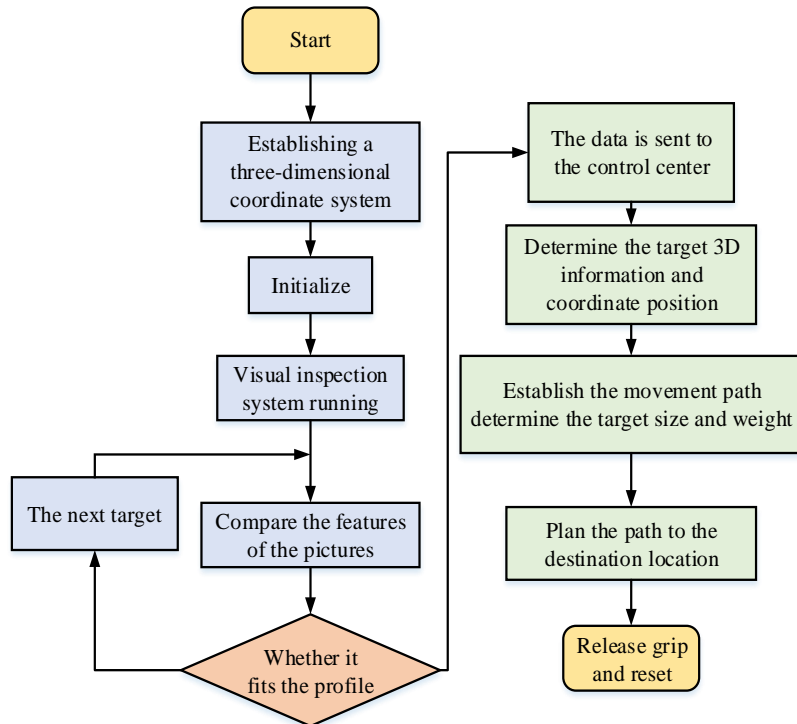

Figure 6: System operation flow chart.

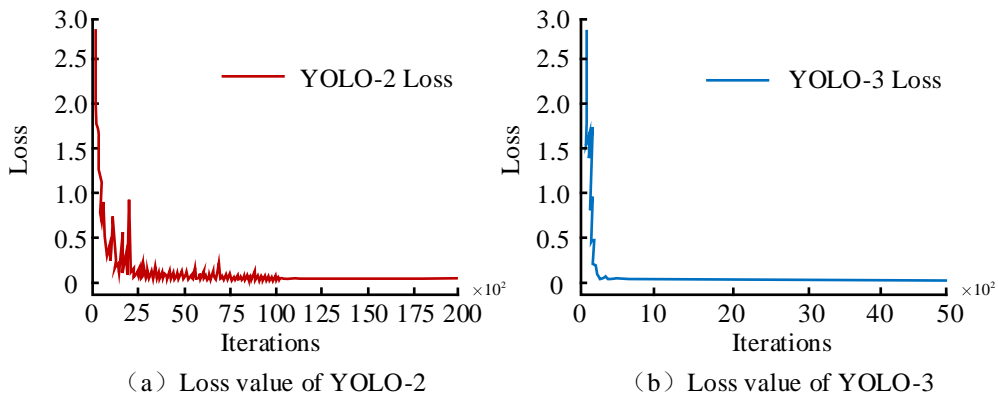（a）Loss value of YOLO-2   （b）Loss value of YOLO-3

Figure 7: The loss curves of YOLO-2 and YOLO-3.

Figure 7 shows the change curve of training loss value of different algorithms. Figure (a) shows the loss curve of the YOLO-2 model. When the iteration times of the model reached 1000 times, the loss value of the YOLO-2 algorithm was about 0.7. Figure (b) shows the loss curve of the YOLO-3 model. When the iteration times reached 1000, the loss value of YOLO-3 reached the

object requirement. And in the iteration process to reach the object loss value, the time consumed by the YOLO-3 was only half that of the YOLO-2. After reaching the object loss value, the YOLO-3 also had a more stable performance in subsequent iterations. Therefore, YOLO-3 had a great advantage in speed and stability. The performance of some typical OD algorithms was compared with the YOLO-3 algorithm proposed in this study. The results are shown in Figure 8.
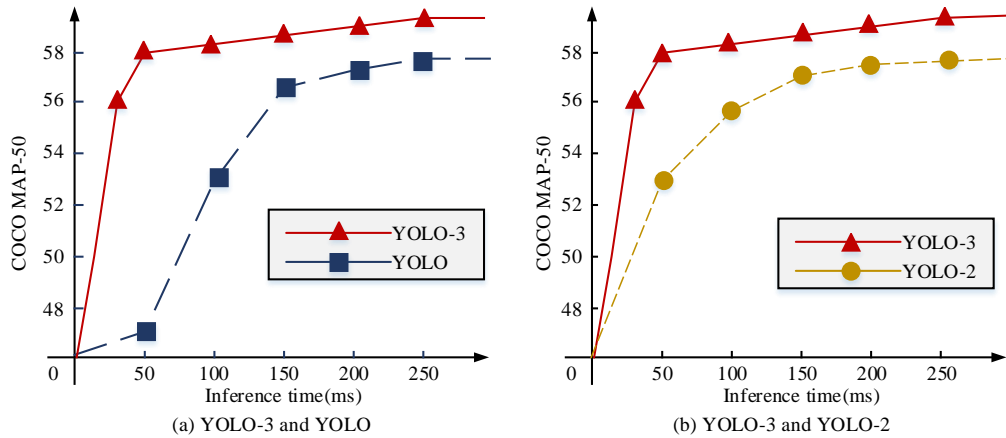
**Figure 8:** Performance comparison of OD models.

From Figure 8, the highest score of YOLO was 57.5, the highest atmosphere of YOLO-2 was 57.8, and the highest score of improved YOLO-3 was 59.2. The accuracy of improved YOLO-3 algorithm on multi-OD was higher than the traditional YOLO and YOLO-2 algorithms. Moreover, when the running time was 50ms, the scores of YOLO and YOLO-2 were below 54, and YOLO is only 47.1. The score of improved YOLO-3 is 58.1 at this time, which is significantly better than the other two types of algorithms. The improved YOLO-3 algorithm proposed in this study not only had higher prediction accuracy, but also faster speed. To further validate the performance of the intelligent MED designed by the study, the ability of the robot arm to recognize the 3D volume information of the object was tested, and five objects with different 3D dimensions, named Object A, Object B, Object C, Object D and Object E, were selected for the experiment. 10 times were detected for each object, and the detection results were recorded and the average and error were calculated. The results are shown in Table 1.

Object A	Length/(cm)	Width/(cm)	Height/(cm)	Volume/(cm3)
Average test value	14.24	7.34	2.45	345.35
Actual value	14.32	7.43	2.41	351.12
Error	0.56%	1.21%	1.66%	1.64%
Object B	Length/(cm)	Width/(cm)	Height/(cm)	Volume/(cm3)
Average test value	8.12	5.16	3.56	275.23
Actual value	8.02	5.23	3.51	268.11
Error	1.25%	1.34%	1.42%	2.66%
Object C	Length/(cm)	Width/(cm)	Height/(cm)	Volume/(cm3)
Average test value	7.22	5.45	4.56	156.23
Actual value	7.29	5.51	4.62	151.28
Error	0.96%	1.09%	1.30%	3.27%

| Object D	Length/(cm)	Width/(cm)	Height/(cm)	Volume/(cm3)
Average test value	11.38	9.34	5.51	445.12
Actual value	11.42	9.29	5.59	446.45
Error	0.35%	0.54%	1.43%	0.30%
Object E	Length/(cm)	Width/(cm)	Height/(cm)	Volume/(cm3)
Average test value	13.13	10.34	3.45	345.98
Actual value	13.19	10.28	3.51	345.87
Error	0.45%	0.58%	1.71%	0.03%

Table 1: Volume calculation results.

From Table 1, the highest error rate in the 3D detection experiments of the object was the volume detection of Object C, which had an increase of 4.95cm3 compared to the actual volume, with an error rate of 3.27%. The lowest error rate was the volume detection of Object E, which had an increase of 0.11cm3 compared to the actual volume, with an error rate of 0.03%. Overall, the measurement errors of the methods proposed in the study were all within 4%. And the average measurement error was 0.71% for length, 0.95% for width, 1.51% for height, and 1.58% for volume. The average error was within 2%, and compared to YOLO and YOLO-2, the method proposed in this study had smaller error. The error of the experimental results for each object is shown in Figure 9.
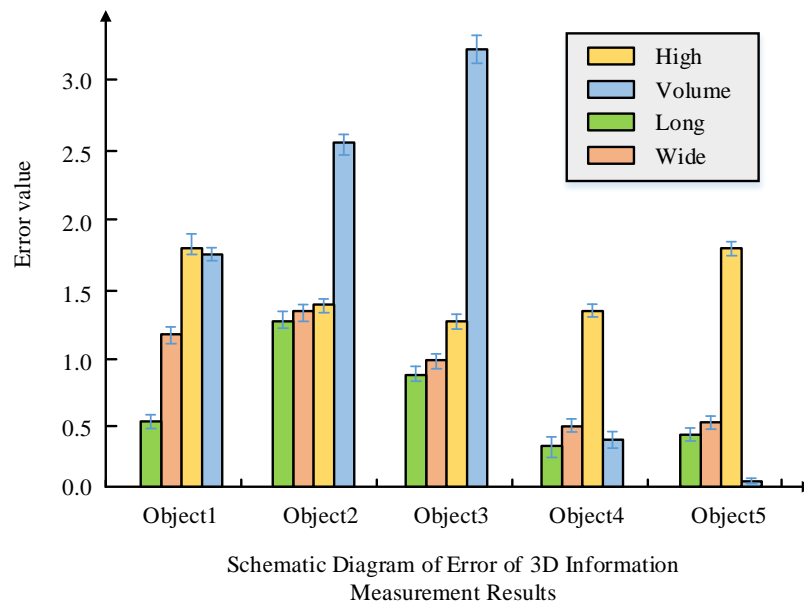
Schematic Diagram of Error of 3D Information
Measurement Results
Figure 9: Experimental result error of each object.

In Figure 9, the method proposed in this study had a much better performance in detecting the length and width of the object with less error. The average error of both length and width was within 1%. In the detection of height and volume, the error of the method proposed in this study was relatively larger, the average detection error of both height and volume was around 1.5%. The intelligent MED system proposed in this study had a more stable performance in the detection of length and width. The identification and detection of objects was an important part in the design

of intelligent mechanical equipment. It determined whether the subsequent manufacturing process can be carried out smoothly. Therefore, although the method proposed in this study had some shortcomings in height and volume measurement, the method proposed in this study was still a better choice compared to other measurement methods. To verify the performance of the intelligent MED system designed in this study in terms of motion planning, the study also set up simulation experiments of the traditional and the new motion planning methods proposed in this paper. The main feature of the motion planning method proposed in this study was fast optimization, i.e., the best optimized path could be obtained quickly as the iteration times increased. The research method was compared with the traditional motion planning method, as shown in Figure 10.
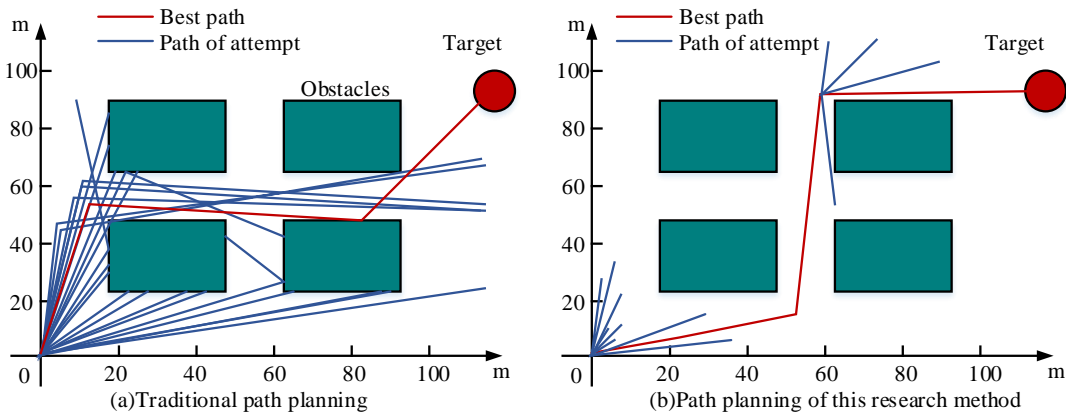
Figure 10: Trajectory planning diagram.

As shown in Figure 10, Figure (a) shows the simulated motion planning of the traditional motion planning method. The traditional motion planning method obtained the final path after 88 iterations. In path selection, the number of previous iterations did not provide a good contribution to subsequent iterations. As a result, the whole iteration process looked unorganized and irregular. Figure (b) represents the motion planning method proposed in this study. After 17 iterations, the final path was obtained by the method proposed in the study, and the paths were mainly long straight lines, concentrated in the initial and focal positions, which can be seen that the previous iteration provides a good directional guidance for the next iteration. Compared with the traditional motion planning method, the optimized path selection method in this study had 71 fewer iterations and performed better in terms of efficiency. The experiments verified that the intelligent MED system based on digital design proposed in this study outperformed other method models at this stage in terms of performance indicators such as accuracy, error rate, speed and efficiency in terms of object identification, detection of 3D information and optimal motion planning.

5 CONCLUSION

The use of digital design technology can provide a big boost to the development of various industries in the country. At present, digital design technology has achieved initial use in the design of intelligent mechanical equipment and remarkable results. Therefore, more scholars have started to optimize digital design technology, aiming to provide a more efficient and accurate method for the design of intelligent mechanical equipment. In this study, based on digital design, the current intelligent MED system was improved by integrating multi-OD algorithms and 3D information detection methods in deep learning. The error control in improving YOLO-3 object 3D recognition was within 4%, and the average measurement errors for length, width, height, and volume in 3D detection were 0.71%, 0.95%, 1.51%, and 1.58%. In the MAP-50 comparative

experiment, YOLO's highest score was 57.5, YOLO-2's highest score was 57.8, and the highest score for improving YOLO-3 was 59.2. And compared to traditional motion planning methods, the proposed method reduced the iteration times required to obtain the optimal path by 80.68%. The method proposed in this study was superior to the current intelligent machinery manufacturing method, had better accuracy, faster running speed, good practical significance and application value. However, the proposed 3D detection model for objects in this study still lacks accuracy in detecting height and volume. At the end of this study, YOLOv7 had achieved faster accuracy improvement, and the use of YOLOv7 may lead to greater progress in research, which will become a key research project in the future.

6   FUTURE WORKS

Intelligent mechanical equipment, which is the core equipment produced in aerospace, automobile manufacturing, rail transportation and other fields, is prone to failure of its key parts such as bearings and gears because it usually serves in high load, high speed, high temperature and other harsh environments. According to statistics, rotating machinery and equipment account for about 80% of the total machinery and equipment, and more than 60% of these mechanical systems or equipment failures are caused by their key components [20]. Therefore, how to effectively process the large amount of mechanical data obtained from sensors to achieve effective monitoring and diagnosis of the health status of mechanical equipment is an urgent need in the industrial field. The application of digital design techniques in the design of intelligent mechanical equipment is an evolving field with numerous possibilities. One of the issues worth further exploration is the real-time adaptation of digital design models. Current models are limited in their ability to adapt to changing manufacturing conditions, with only 20-30% of models reporting real-time adaptation [21]. It needs to develop digital design algorithms that can adapt to the dynamic characteristics of intelligent mechanical systems. Moreover, manufacturing accounts for more than 30% of the world's energy consumption, and the development of sustainable intelligent mechanical systems using digital design techniques is a highly promising direction to explore [22]. Future research can focus on optimizing digital design algorithms to minimize energy consumption and promote sustainability in manufacturing.

Qiujing Meng, http://orcid.org/0009-0002-0368-7197

REFERENCES

[1]   Chen, Y.; Long, J.; Shi, D.; Chen, X.; Hou, M.; Gao, J.; Liu, H.; He, Y.; Fan, B.: Achieving a sub-10 nm Nanopore Array in Silicon by Metal-assisted Chemical Etching and Machine Learning, International Journal of Extreme Manufacturing, 3(3), 2021, 83-93. https://doi.org/10.1088/2631-7990/abff6a

[2]   Quan, Z. A.; Rm, A.; Yue, H. B.; Lu, Z. A.; Zhen, Z. C.: Measurement of Sustainable Development Index in China's Manufacturing Industry based on Er-xiang Dual theory, Alexandria Engineering Journal, 60(6), 2021, 5897-5908. https://doi.org/10.1016/j.aej.2021.04.003

[3]   Doran, M.; Nugent-Folan, G.: Digitized Beckett: Samuel Beckett's Self-Translation Praxes Mediated through Digital Technology, Anglia, 139(1), 2021, 181-194. https://doi.org/10.1515/ang-2021-0009

[4]   Ms, A.; Drs, B.: How Globalization is Changing Digital Technology Adoption: An International Perspective, Journal of Innovation & Knowledge, 6(4), 2021, 222-233. https://doi.org/10.1016/j.jik.2021.04.001

[5]   Zheng, Z.; Lei, L.; Sun, H.; Kuang, G.: FAGNet: Multi-Scale Object Detection Method in Remote Sensing Images by Combining MAFPN and GVR, Journal of Computer- Aided Design & Computer Graphics, 33(6), 2021, 883-894. https://doi.org/10.3724/SP.J.1089.2021.18608

[6]   Ae, A.; Bs, A.; Jlq, B.; Cdp, B.; Zkn, A.: Optimization-based Digital Design of a Commercial Pharmaceutical Crystallization Process for Size and Shape Control, European Symposium on Computer Aided Process Engineering, 50(31), 2021, 1143-1148. https://doi.org/10.1016/B978-0-323-88506-5.50176-5

[7]   Cheung, K. L.; Hors-Fraile, S.; Vries, H.: How to Use the Integrated-Change Model to Design Digital Health Programs – ScienceDirect, Digital Health, 1(8), 2021, 143-157. https://doi.org/10.1016/B978-0-12-820077-3.00008-0

[8]   Zhou, J.; Barati, B.; Wu, J.; Scherer, D.; Karana, E.: Digital Biofabrication to Realize the Potentials of Plant Roots for Product Design, Bio-Design and Manufacturing, 4(1), 2021, 111-122. https://doi.org/10.1007/s42242-020-00088-2

[10]   Charavet, C.; Bernard, J.; Gaillard, C.; Gall, M.: Digital Smile Design (DSD): A Complementary Digital Protocol Used for the Planning of Orthodontic Treatment, Revue d'Orthopédie Dento-Faciale, 53(3), 2019, 263-270. https://doi.org/10.1016/j.ortho.2019.06.019

[11]   Choudhary, M.; Tiwari, V.; Uduthalapally, V.: Iris presentation attack detection based on best-kfeature selection from YOLO inspired RoI, Neural Computing & Applications, 33(11), 2021, 5609-5629. https://doi.org/10.1007/s00521-020-05342-3

[12]   Shen, H.; Dong, Z.; Yan. Y.; Fan, R.; Jiang, Y.; Chen, Z.; Chen, D.: Building roof extraction from ASTIL echo images applying OSA-YOLOv5s, Applied Optics, 2022, 61(11), 2923-2928. https://doi.org/10.1364/AO.451245

[13]   Dasygenis, M.: Design and Implementation of a Robotic Arm Assistant with Voice Interaction Using Machine Vision, Automation, 2(4), 2021, 238-251. https://doi.org/10.3390/automation2040015

[14]   Li, D.; Liu, H.; Wei, T.; Zhou, J.: Robotic grasping method of bolster spring based on image-based visual servoing with YOLOv3 object detection algorithm, Proceedings of the Institution of Mechanical Engineers, Part C: Journal of Mechanical Engineering Science, 236(3), 2022, 1780-1795. https://doi.org/10.1177/09544062211019774

[15]   Hadzi-Velkov, Z.; Pejoski, S.; Zlatanov, N.; Gacanin, H.: Designing Wireless Powered Networks Assisted by Intelligent Reflecting Surfaces with Mechanical Tilt, IEEE Communications Letters, 25(10), 2021, 3355-3359. https://doi.org/10.1109/LCOMM.2021.3098128

[16]   Fei, W.; Meng-ting, L.; Xue-qin, L Zhi-liang, Q.; Ben-jun, M.; Yi, Z.: Real-time Detection of Marine Vessels under Sea Fog Weather Conditions based on YOLOv3 Deep Learning, Marine Sciences, 44(8), 2022,197-204. https://doi.org/ 10.11759/hykx20200106001

[17]   Yang, B.; Wang, J.: An Improved Helmet Detection Algorithm Based on YOLO V4, International Journal of Foundations of Computer Science, 33(7), 2022, 887-902. https://doi.org/10.1142/S0129054122420205

[18]   Won-Jae, L.; Myung-Il, R.; Hye-Won, L.; Jisang, H.; Yeong-Min, C.; Sung-Jun, L.; Sun, S.: Detection and Tracking for the Awareness of Surroundings of a Ship based on Deep Learning, Journal of Computational Design and Engineering, 5(5), 2021, 1407-1430. https://doi.org/10.1093/jcde/qwab053

[19]   Gautam, Y.; Prajapati, B.; Dhakal, S.; Pandeya, B.; Prajapati, B.: Vision-based Intelligent Path Planning for SCARA Arm, Cognitive Robotics, 1(1), 2021, 168-181. https://doi.org/10.1016/j.cogr.2021.09.002

[20]   Shoujiang, Z.; Fan, L.; Peng, Y.; Hongying, Z.; Anang, A.: Microlens Light Field Imaging Method Based on Bionic Vision and 3-3 Dimensional Information Transforming, Journal of Geodesy and Geoinformation Science, 2(2), 2019, 72-79. https://doi.org/CNKI:SUN:CHBX.0.2019-02-008

[21]   Guo, Q.; Li, Y.; Liu, Y.; Gao, S.; Song, Y.: Data augmentation for intelligent mechanical fault diagnosis based on local shared multiple-generator GAN, IEEE Sensors Journal, 22(10), 2022, 9598-9609. https://doi.org/10.1109/JSEN.2022.3163658

[22] Qian, C.; Zhu, J.; Shen, Y.; Jiang, Q.; Zhang, Q.: Deep transfer learning in mechanical intelligent fault diagnosis: application and challenge, Neural Processing Letters, 54(3), 2022, 2509-2531. https://doi.org/10.1007/s11063-021-10719-z

[23] Zhu, J.; Jiang, Q.; Shen, Y.; Qian, C.; Xu, F.; Zhu, Q.: Application of recurrent neural network to mechanical fault diagnosis: A review, Journal of Mechanical Science and Technology, 36(2), 2022, 527-542. https://doi.org/10.1007/s12206-022-0102-1